






Cite this: *Soft Matter*, 2021,  
17, 715

# Metal cation responsive anionic microgels: behaviour towards biologically relevant divalent and trivalent ions†

Vittoria Chimisso,  Simona Conti, Phally Kong, Csaba Fodor  and  
Wolfgang P. Meier \*

Anionic poly(vinylcaprolactam-co-itaconicacid-co-dimethylitaconate) microgels were synthesized via dispersion polymerization and their responsiveness towards cations, namely  $\text{Mg}^{2+}$ ,  $\text{Sr}^{2+}$ ,  $\text{Cu}^{2+}$  and  $\text{Fe}^{3+}$ , was investigated. The itaconic moieties chelate the metal ions which act as a crosslinker and decrease the electrostatic repulsion within the network, leading to a decrease in the gel size. The responsiveness towards the metal ion concentration has been studied via dynamic light scattering (DLS) and the number of ions bonded within the network has been quantified with ion chromatography. Through the protonation of the carboxylate groups in the gel network, their interaction with the cations is significantly lowered, and the metals are consequently released back in solution. The number of ions released was assessed also via ion chromatography for all four ions, whilst  $\text{Mg}^{2+}$  was also used as a model ion to display the reversibility of the system. The microgels can bond and release divalent cations over multiple cycles without undergoing any loss of functionality. Moreover, these gels also selectively entrap  $\text{Fe}^{3+}$  with respect to the remaining divalent cations, opening the possibility of using the proposed gels in the digestive tract as biocompatible chelating agents to fight iron overaccumulation.

Received 10th August 2020,  
Accepted 1st October 2020

DOI: 10.1039/d0sm01458c

[rsc.li/soft-matter-journal](http://rsc.li/soft-matter-journal)

## Introduction

Divalent and trivalent metal cations are of crucial importance in the elapse of biochemical reactions within the body, yet can also act as toxic agents when they exceed physiological concentrations in the system.<sup>1,2</sup> For instance, some metals such as  $\text{Cu}^{2+}$  and  $\text{Pb}^{2+}$  are commonly known as pollutants due to their elevated toxicity in the body even at minimal concentrations, whilst other metals like  $\text{Fe}^{3+}$ , generally not harmful, can also lead to long-term damage when pre-existing conditions are present, such as  $\beta$ -thalassemia or diabetes.<sup>3–5</sup> The uncontrolled accumulation of metal ions or toxins in the body can lead to oxidative stress and cell damage, and their removal requires invasive and long therapies, such as injections of chelating agents and dialyses, multiple times a day.<sup>5,6</sup> The most common and effective chelating agent used in these therapies is ethylenediaminetetraacetic acid (EDTA), which however has the major drawback to bond  $\text{Ca}^{2+}$ . The use of EDTA is linked thus to hypocalcaemia in a patient as well as bone resorption.<sup>7</sup> This drawback has been positively exploited by Karamched *et al.*, where they presented anti-elastin decorated albumin nanoparticles

loaded with EDTA, which would bond  $\text{Ca}^{2+}$  and reduce calcification in patients with chronic kidney disease.<sup>8</sup>

An alternative way to remove the ions from the body is to prevent them from entering the blood stream when ingested. This can be achieved through a sequestrant of the targeted metal ion within the digestive track that can be expelled through it whilst carrying the toxic ion, so as to avoid intravenous injections, which might have a toll on the body. Commercial polymers of this kind are already available, and one prominent example is Kayexalate<sup>®</sup>, which is widely employed to fight hyperpotassaemia. However, its use also leads to strong side effects such as bleeding and intestinal necrosis when assumed in combination with sorbitol. Hence, the need to reduce the interaction of the active moieties with soft tissues suggests the use of more complex polymer architectures, namely gels and microgels. Positively charged metal ions bond strongly to electron donating ligands such as amines, carboxyl groups, thiols and hydroxyl groups.<sup>9,10</sup> The cations can thus be entrapped within a material by designing cross-linked polymer networks decorated with the mentioned functional groups, which act as scavengers for the metal cation.<sup>11–15</sup> The simplicity of these systems allows elegant production of materials that selectively entrap a specific ion, generally a pollutant, such as  $\text{Pb}^{2+}$  or  $\text{Hg}^{2+}$ .<sup>16</sup> There are plenty of examples in which negatively charged hydrogels or polymeric membranes have been used as water purification systems.<sup>17,18</sup>

Department of Chemistry, University of Basel, Mattenstrasse 24/a, 4002, Basel, Switzerland. E-mail: [wolfgang.meier@unibas.ch](mailto:wolfgang.meier@unibas.ch)

† Electronic supplementary information (ESI) available. See DOI: 10.1039/d0sm01458c



However, due to their larger dimensions and poor mechanical properties of crosslinked gels, they are less versatile for *in vivo* applications in terms of ion removal. The only gels that find wider soft tissue applications are supramolecular gels, which are injectable within the body, as they are both shear thinning and self-healing.<sup>19,20</sup> Despite their versatility, these gels have been proven so far to be excellent candidates for tissue scaffolding or drug delivery but their behaviour in terms of ion uptake/release has been overseen.<sup>21</sup> Sizing down to the micro and nano metre scale these gels access another class of soft materials, commonly known as microgels.<sup>22</sup> These gels, which normally range from 10 nm to 1  $\mu$ m, provide soft, deformable and highly porous nanoparticles with high biocompatibility together with extensive chemical versatility, as they are composed of the same polymeric chains of their macroscopic counterparts.<sup>22</sup> Designing these gels to be responsive to external stimuli such as temperature or pH introduces the possibility of taking up or releasing “on demand” a cargo such as a small molecule, a polyelectrolyte or a metal cation.<sup>23,24</sup> Taking up and coordinating a metal ion (alkali, earth alkali or transition) induces the hydrogel to shrink and expel water, due to an interplay between charge screening, charge correlation, and, in the case of transition metals, additional crosslinking. There are extensive and very precise studies on macroscopic polyelectrolyte gels interacting with divalent and trivalent metal cations, both experimental and theoretical models.<sup>25</sup> However, even though these contributions present accurate explanation on the coordination and thermodynamics of swelling, they do not provide quantification of ion uptake and release by an external stimulus other than an excessive ionic strength, nor competition between different biologically relevant divalent ions (addition of  $\text{Na}^+$ ). Previously, we have shown that by using microgels composed of vinylcaprolactam (VCL) and itaconic acid (IA) we could design a system that is stable at physiological temperature (36–38 °C), biocompatible and able to uptake and release  $\text{Ca}^{2+}$  ions upon pH changes.<sup>26,27</sup>

The possibility of quantitatively removing ions from the aqueous environment had been investigated only for  $\text{Ca}^{2+}$ , excluding other ions that can play a role in biochemical reactions (such as  $\text{Fe}^{3+}$  or  $\text{Sr}^{2+}$ ), trigger polymerisations ( $\text{Mg}^{2+}$ ) such as the polymerisation of G-actin into F-actin or might be hazardous ( $\text{Cu}^{2+}$ ).<sup>28,29</sup> Herein, we have tested the ability of the gel systems to capture metal ions and to release them with dependence on pH changes. Furthermore, tests were made for a series of biologically relevant ions, which are potentially toxic for the body, and show how these gel systems can be captured, stored and eventually cleaned for reuse. One potential application of these gels would be their use in chelation therapy *via* oral administration instead of a direct injection into the bloodstream.

## Experimental

### Materials

N-Vinylcaprolactam (VCL, 98%) was purchased from Sigma-Aldrich and purified *via* reduced pressure distillation. Dimethylitaconate (IADME, 99%), *N,N'*-methylene(bis)acrylamide (BIS, 99%),

**Table 1** Molar composition, mol% of crosslinker and molar% of COOH in microgels M1, M2 and M3, determined *via* potentiometric titration

Microgel	Mol% VCL	Mol% BIS	Mol% COOH
M1	95	2.5	5.8
M2	90	2.5	10
M3	85	2.5	18

hexadecyltrimethylammonium bromide (CTAB, 99%), magnesium chloride ( $\text{MgCl}_2 \cdot 6\text{H}_2\text{O}$ ), strontium chloride ( $\text{SrCl}_2 \cdot 4\text{H}_2\text{O}$ , 99%), copper chloride ( $\text{CuCl}_2 \cdot 6\text{H}_2\text{O}$ , 99%), iron chloride ( $\text{FeCl}_3$  anhydrous, 99%), uranyl acetate (>99%) and sodium phosphotungstate hydrate (PTA > 99%) were purchased from Sigma Aldrich and used as received. 2'-Azobis(2-methylpropionamide)dihydrochloride (AMPA, granular, 97%) was purchased from Acros Organic. Hydrochloric acid stock solution (HCl, 1 M), sodium hydroxide stock solution (NaOH 1 M and 0.01 M) and nitric acid ( $\text{HNO}_3$ , 12 M) were purchased from Merck. Phosphate buffer saline solution (PBS, without  $\text{Ca}^{2+}$  and  $\text{Mg}^{2+}$ ) was acquired from Dulbecco. Deuterated chloroform ( $\text{CDCl}_3$ ) and deuterated water ( $\text{D}_2\text{O}$ ) were obtained from Cambridge Isotope Laboratories, Inc. All experiments were performed using Millipore water filtered over a 0.450  $\mu\text{m}$  regenerated cellulose filter with a resistivity of 18  $\text{M}\Omega \text{ cm}^{-1}$  at neutral pH and in the absence of buffer. Each metal ion solution used was made by dissolving the hydrated solid ion powder into degassed MilliQ water at RT to a final concentration of 100 mM, and used as stock solutions and the exact concentration was measured by ion chromatography (Table 1).

### Sample identification

The neutral microgels P(VCL-*co*-IADME) are identified with  $Nn$  ( $n = 0, 1, 2$  and 3) describing a respective amount of IADME mol% of 0, 5, 10 and 20. The hydrolysed microgels P(VCL-*co*-IADME-*co*-IA) are named  $Mn$  ( $n = 1, 2$  and 3) which are the respective hydrolysed microgels of the  $N$  microgel samples, with a respective amount of COOH mol% of 5.8, 10 and 18.

## Methods

### Synthesis of P(VCL-*co*-IADME) microgels

Microgels were prepared according to the previously described procedure.<sup>26,30</sup> An aqueous stock solution of BIS and CTAB was prepared, and appropriate amounts of water, VCL and IADME were added to the solution mixture (140 mL) in a three neck round bottom flask, equipped with a thermometer, a mechanical stirrer and a syringe. The respective amounts of VCL, IADME, BIS and CTAB are listed in Table S1 (see in the ESI†) to obtain the microgels in 5, 10 and 15 mol% of IADME (M1, M2 and M3 respectively). The mixture was then degassed by being purged with dry nitrogen for 60 min at a 300 rpm stirring rate whilst being heated up to 70 °C. After 1 h, an aqueous solution of AMPA (10 mL) was prepared and equally degassed for a minimum of 10 min at room temperature (RT). The polymerization was initiated by adding in one shot the initiator solution to the warm reaction mixture. The reaction was allowed to proceed at 70 °C for 4 h, before being quenched



with the addition of air to the reaction vessel and by allowing the reaction mixture to cool down to RT. The microgels were purified *via* dialysis (Spectra/Por<sup>®</sup> 7 Dialysis Membrane, Pre-treated RC tubing, MWCO: 50 kDa) against MilliQ water for 6 days, with frequent water exchange. To determine the wt% of the solution, 2 mL of gel solution was lyophilized for 3 days and its dry weight was measured with an analytical scale. The gels were stored as aqueous stock solutions at RT for further use.

#### Hydrolysis of P(VCL-co-IADME) microgels to obtain P(VCL-co-IADME-co-IA) microgels

A sample of microgel solution was diluted with 1 M NaOH to a final concentration of 0.1 M and was left stirring at RT for 6 days. The microgels were then purified *via* dialysis (Spectra/Por<sup>®</sup> 7 Dialysis Membrane, Pre-treated RC tubing, MWCO: 50 kDa) against Millipore water for 2 days, with frequent water exchange and stored as stock solutions at RT for further use. In order to determine the weight content of the solution, 2 mL of microgel solution was lyophilized for 3 days and weighed on a high precision analytical scale.

#### Cation triggered gel collapse

Each microgel sample (M1, M2 and M3) was dispersed in a solution of  $M^{n+}$  ions at several concentrations (100, 10, 1, 0.5, 0.1, 0.05, 0.01, 0.001 and 0.0001 mM) to a final concentration of 0.02 wt% of microgels at neutral pH. The diameter collapse was measured *via* dynamic light scattering.

#### Cation loading experiment

In order to load a microgel sample with a certain cation, an aqueous mixture of 0.1 wt% of microgel and 1 mM of ion were obtained (at RT and neutral pH), and left equilibrating under agitation overnight. The samples were subjected to centrifugation in a VIVASPIN 20<sup>®</sup> at 2000 rpm for 60 min, to obtain a microgel free filtrate which was collected for analysis. The concentrated microgel solution was diluted to a final volume of 5 mL with MilliQ water and used for further experiments.

#### Cation leaching experiment

The microgel solution was loaded in the same manner as stated previously and subjected to 10 cycles of centrifugation (4 min, 2000 rpm) and at each cycle they were redispersed in fresh Millipore water. Each filtrate was collected and analysed by ion chromatography.

#### Cation release experiment

A microgel sample (5 mL, 0.1 wt%, pH = 7) was loaded and washed with Millipore water, and subsequently centrifuged to reduce the volume of the microgel solution (40 min, 2000 rpm). The concentrated solution was diluted with 1 M HCl and MilliQ water to equilibrate it to the desired pH (2, 3, 4, 5 and 6) to a final volume of 5 mL at RT. The sample was then left equilibrating on a shaker for 10 minutes and centrifuged with a VIVASPIN 20<sup>®</sup> centrifuge filter (Sartorius Stedim biotech, VIVASPIN 20<sup>®</sup>, MWCO PES: 10 kDa) for 40 min at 2000 rpm. The microgel free filtrate was collected and analysed by ion chromatography.

#### System reversibility experiment

To determine whether the loading and unloading of a microgel system is reversible, the reversibility test was performed. The reversibility experiment involved  $Mg^{2+}$  loading into a 5 mL 0.1 wt% microgel solution at pH 7 and RT in a VIVASPIN 20<sup>®</sup> centrifuge filter (Sartorius Stedim biotech, Vivaspin 20<sup>®</sup>, MWCO PES: 10 kDa) and equilibration of the sample for 2 h. The sample was centrifuged and washed with MilliQ water, and redispersed to a final volume of 5 mL. The pH of the sample was subsequently lowered to 2 with 1 M HCl, and the microgel solution was left equilibrating for 2 h at RT. The sample was then centrifuged (40 min, 2000 rpm), and subjected to dispersion in MilliQ water three times at pH 7 and RT for 2 h and centrifugation (40 min, 2000 rpm). Each microgel free filtrate was collected and analysed *via* ion chromatography. The above-mentioned cycle was repeated three times.

#### Competition between metal ions

To describe the selectivity of the uptake of a certain ion  $M^{n+}$  ( $Mg^{2+}$ ,  $Sr^{2+}$ ,  $Cu^{2+}$  and  $Fe^{3+}$ ) solutions containing the same number of different metal ions were mixed with a microgel solution to a final volume of 5 mL, a final  $M^{n+}$  concentration of 1 mM for each ion and a final microgel concentration of 0.1 wt%. The gels were left equilibrating overnight on a shaker at RT and neutral pH and subsequently centrifuged with a VIVASPIN 20<sup>®</sup> centrifuge filter (Sartorius Stedim biotech, Vivaspin 20, MWCO PES: 10 kDa), and the filtrate was collected for analysis. The number of  $M^{n+}$  ions bonded was determined by ion chromatography.

#### Ion chromatography (IC)

The amount of  $M^{n+}$  bonded, retained or released was measured quantitatively with a 940 professional IC Vario (Metrohm Germany). Each microgel filtrate was diluted 1:5 with  $HNO_3$  and 1 ppm  $Y^{3+}$ . 30  $\mu$ L of centrifuged sample were eluted on a 250  $\times$  40 mm<sup>2</sup> column with an elution flux of 0.8 mL min<sup>-1</sup> in  $HNO_3$  (7.25 mM) at 30 °C. Each datapoint shown is a result of three independent measurement averages.

#### Light scattering (LS)

Dynamic light scattering (DLS) was used to determine the hydrodynamic diameter ( $D_H$ ) of each microgel sample under different conditions.  $D_H$  was measured with a Zetasizer Nano ZsP (Malvern Instruments, Germany). Each measurement was taken at 20 °C, after an equilibration time of 300 s with a backscattering angle of 173°. Static light scattering (SLS) was used for pH dependent measurements to determine the radius of gyration ( $R_g$ ) which were taken with a LS spectrometer (LS Instruments, Switzerland) equipped with a HeNe laser (633 nm) with varying scattering angles (30–135°) in the 2D/pseudo cross-correlation mode.

#### Transmission electron microscopy (TEM)

The dried morphology of the microgels was imaged by TEM with a Philips Morgagni 268D microscope. Microgel solutions



in water (0.01 wt%) were negatively stained with a solution of 0.015% of uranyl acetate and deposited on a carbon copper grid.

### Potentiometric titration

The amount of COOH groups in each microgel sample was determined with potentiometric titration and the  $pK_a$  values were evaluated in the pH range of 5–9 using a Zetasizer Nano ZsP (Malvern Instruments, United Kingdom). The titration involved 0.1 wt% microgel solutions in water using a MPT-2 multipurpose titrator (Malvern Instruments, United Kingdom) with a MV114-SC Malvern Comb Glass Electrode. The aqueous solutions were titrated with NaOH (0.01 M) at intervals with increment of 0.5. The zeta ( $\zeta$ )-potential was also determined at pH 7 at RT, on an average of three independent measurements. The data collected were processed through the Zetasizer Software (v7.0) (Malvern Instruments, United Kingdom).

## Results and discussion

### Microgel synthesis and characterization

M1, M2 and M3 were synthesized in a two-step approach *via* dispersion polymerization.<sup>26</sup> First, neutral microgels composed of VCL and IADME were produced and purified *via* dialysis (see Table S1 in the ESI†). The gels were subsequently treated with 0.1 M NaOH to ensure the hydrolysis of the COOMe groups of the IADME monomer into its corresponding carboxyl group, which will act as a metal ion scavenger. In order to determine the chemical composition of Mn, a combination of techniques involving <sup>1</sup>H NMR and potentiometric titration was used (see Table S2 in the ESI†). TEM was utilised to determine the dry morphology of the gels (Fig. 1). As already shown in previous publication, due to the higher reactivity of IADME compared to VCL, the core of the microgel is richer in COOH groups. This can be clearly observed in the TEM image (Fig. 1): the uranyl

acetate is positively charged and will preferably stain the COOH groups within the gel.<sup>26</sup> Their swollen diameter in water was measured *via* DLS, where M1 is characterized by  $D_H = (400 \pm 20)$  nm, M2 by  $D_H = (430 \pm 15)$  nm and M3 by  $D_H = (480 \pm 20)$  nm. Since also the crosslinker is more reactive than VCL, its accumulation within the microgel core is expected.<sup>30</sup> The  $R_g/R_H$  ratio of around 0.45 confirms a denser core that becomes less crosslinked in its periphery (see Table S3 in the ESI†).<sup>23</sup> In all gels the structure appears to be consistent with that previously reported, showing a structure characterised by a denser core decorated by dangling chains in its corona. The structure shifts towards a hard sphere ( $R_g/R_H$  increases to 0.6) in the presence of ions (see Table S3 in the ESI†), since the interchain repulsion decreases in the presence of metals that screen the negative charges coming from the COO<sup>−</sup> moieties. The gel diameter decreases to a higher extent at low pH (below pH 3), when all carboxylate ions could be protonated into COOH, whilst maintaining the same  $R_g/R_H$  ratio. In fact, the  $R_g/R_H$  ratio for protonated gels has an average value for all gels comparable to the  $R_g/R_H$  ratio of the one that is obtained for the gels in 1 mM M<sup>n+</sup> solution. This suggests that even if the microgels shrink, by expelling water from their network, due to the protonation of the COOH groups, the structure of the internal organization remains the same. The major structural change of the gels is observed between the gels under neutral conditions, in which they are deprotonated and the network is fully expanded by the solvent, and the metal containing or protonated gels, where the amount of solvent, water, is drastically reduced yet still present. By collapsing the gels upon addition of cations or acid, there is an initial collapse of the outer, less cross-linked, corona, followed by shrinkage of the core. This is accountable to the difference in crosslinking density between the core and the microgel corona, due to a more consistent presence of the cross-linker in the centre of the microgel, which accounts for a local stiffness of the gel structure.

### Ion triggered microgel collapse

The responsiveness of the microgels towards the ion concentration has been investigated with DLS. As it is apparent from Fig. 2, the gels are swollen at low ion concentration and start deswelling in the concentration range of 0.05–0.1 mM. The metal ion concentration at which the gel structure shrinks by expelling water from its network is slightly dependent on the nature of the ion. In fact, in all microgel systems, regardless of the ion they are interacting with, the  $D_H$  size starts to decrease at a metal concentration of 0.05 mM. The size dispersity also accordingly decreases as it is apparent from a substantial reduction of the error bars for each data point in Fig. 2, hinting a more compact structure, which is confirmed by the  $R_g/R_H$  ratio measured for each gel at a metal concentration of 1 mM (see Table S3 in the ESI†). On the other hand, the concentration range at which the microgels decrease drastically their size is narrower in the case of the transition metal ions, especially in the case of Fe<sup>3+</sup>, where the collapse of the gel occurs between Fe<sup>3+</sup> concentrations of 0.05 and 0.1 mM. When multivalent cations are added to the systems, they can influence the intermolecular

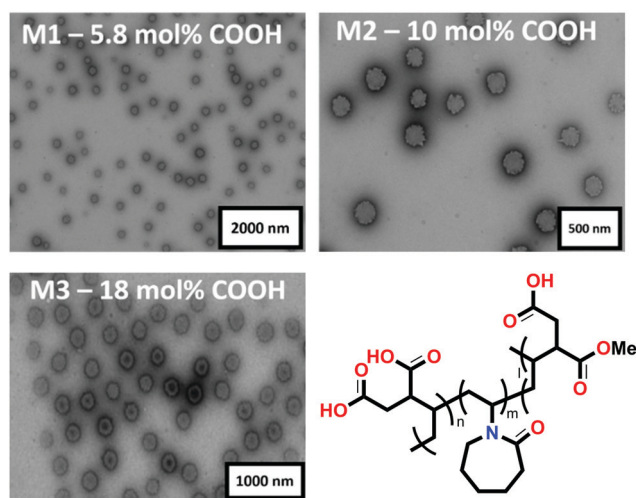


Fig. 1 TEM images of M1 (5.8 mol% COOH), M2 (10 mol% COOH) and M3 (18 mol% COOH) VCL based microgels at neutral pH stained with uranyl acetate. Schematic representation of the chemical composition of Mn microgels.





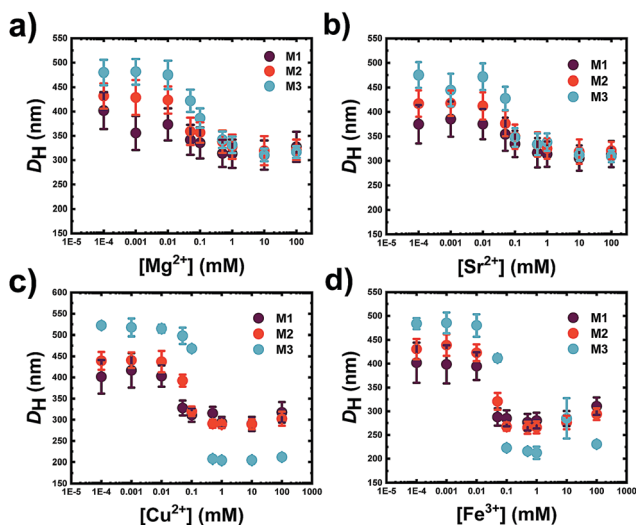


Fig. 2 Hydrodynamic diameter ( $D_H$ ) of M1 (5.8 mol% COOH), M2 (10 mol% COOH) and M3 (18 mol% COOH) at different (a)  $Mg^{2+}$ , (b)  $Sr^{2+}$ , (c)  $Cu^{2+}$  and (d)  $Fe^{3+}$  taken at RT in MilliQ water at neutral pH.

chain-chain interaction by correlation between the  $COO^-$  charges and the cation, driving the charged chains closer to each other, leading to network shrinkage. Moreover, they can also screen the negative charges associated with the  $COO^-$  groups, thus reducing the interchain electrostatic repulsion.<sup>31,32</sup> Moreover, rheological data on weak polyelectrolyte macroscopic hydrogels have shown that earth alkali ions are not capable of forming cross-links, as the storage modulus of gels containing either  $M^{2+}$  or  $M^+$  metals was not significantly different. In contrast, the presence of transition metals increased the shear modulus of the PE gel, suggesting an additional interaction of the metals with the network that goes beyond charge correlation and involves the formation of coordination complexes.<sup>25</sup> According to the electronic configuration of the ion, this can screen and coordinate the functional groups of the gel differently. By looking at the changes in swelling of the same gel at the same ion concentration, the  $D_H$  changes according to the metal ion used. When an alkaline earth metal ion is present, gels normally shrink to an average size of 300 nm, losing from 20 to 40% of the  $D_H$ , whilst transition metal ions lead to a decrease in  $D_H$  up to 60%. Therefore, the coordination between carboxyl groups increases in the presence of transition metal ions. On one hand, the alkaline earth ions  $Mg^{2+}$  and  $Sr^{2+}$  trigger the collapse of the microgel to the same extent: in both cases, the final  $D_H$  is around 300 nm. On the other hand, the presence of transition metal ions triggers a stronger collapse of the network, possibly due to the coordination capacity of the given metal ions. The oxidation number does not seem to influence the swelling degree in charged gels as both ions lead to a final  $D_H$  of M3 of 200 nm. Former studies have investigated the swelling behaviour of macroscopic weak PE gels in the presence of divalent earth alkali and transition metal cations.<sup>25</sup> Interestingly, one study observes a sharp transition from the swollen to the shrunken state of the gel with COOH mol% of 100% in macroscopic gels in the presence of  $CaCl_2$ , whilst gels containing up to 40 mol% of charged groups present a continuous

phase transition.<sup>33</sup> This threshold is, as it is clear from Fig. 2c and d, significantly lowered in the case of microgels, where 10 mol% of COOH moieties are enough to fully collapse the gel network upon a critical cation concentration change. These experimental findings are in agreement with those predicted in simulations by Jha *et al.*<sup>34</sup> By exploring the swelling behaviour of homopolymeric VCL microgels (N0) in the presence of divalent ions, all these seem to shrink in the presence of a higher ionic strength, yet not as strongly as in the case of the anionic systems (see Table S4 in the ESI†).  $Fe^{3+}$  on the other hand leads not only to a decrease in  $D_H$  of N0 but also to an increase of dispersity of the sample, suggesting that aggregation takes place in solution, whilst the same microgel solution remains stable in the presence of the remaining ions, see Table S4 in the ESI†. This might suggest a coordination of the metal ions with the lactam groups of the gel rather than with the COOH groups.<sup>32</sup> By exchanging the divalent ions with monovalent ones such as  $Na^+$ , the effect observed towards the swelling behaviour of each gel is similar to the one observed in the presence of divalent ions. In fact, both ions, when at concentrations higher than 1 mM, trigger the collapse of the gels. However, as seen in Fig. 3, a sharper change in the swelling ratio between the collapsed state and the swollen state is observed with  $M^{2+}$ . At the same ion concentration, the ionic strength of a  $M^{2+}$  or  $M^{3+}$  is respectively 4 times or 9 times higher than the one associated with an  $M^+$  solution. This suggests that the influence of the ionic strength is negligible in that area, and the collapse of the network is mostly due to the screened interaction among the  $COO^-$  charges by the doubly charged ion, which leads to a reduced electrostatic repulsion.<sup>35</sup> Moreover,  $Mg^{2+}$  as other divalent metal cations can act as a supramolecular cross-linker between the  $COO^-$  groups if they are in close proximity to each other by correlating its charges with the ones belonging to  $COO^-$ . In Fig. 3, the collapse of the same microgel is much more abrupt in the presence of  $Mg^{2+}$  in the range of 0.01 M and 100 mM. At very high molar concentrations, the  $D_H$  of the gels is then again comparable, suggesting that the ionic strength becomes the predominant factor to influence the  $D_H$  of the gels.

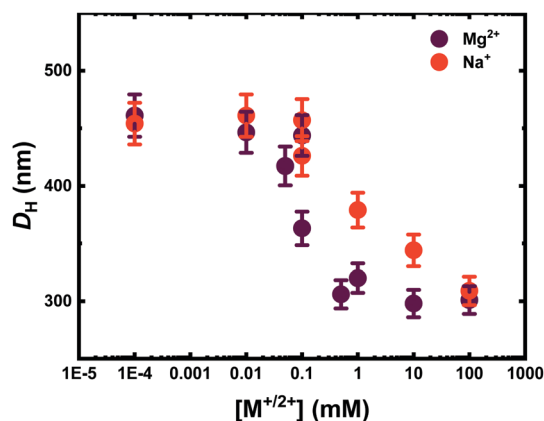


Fig. 3 Hydrodynamic diameter  $D_H$  of M2 (10 mol% COOH) measured via DLS in the presence of  $Mg^{2+}$  (purple) and  $Na^+$  (red) in MilliQ water, at neutral pH and RT.



### Ion uptake and pH dependent release

The number of ions coordinated by a 0.1 wt% solution of microgels at different COOH mol% is shown in Fig. 4. Clearly, the number of ions coordinated by the P(VCL-co-IADME-co-IA) microgel network is dependent on the amount of COOH present. However, if the presence of COOH groups is fundamental to coordinate the alkaline earth ions and  $\text{Cu}^{2+}$ , it does seem to play a rather minor role for  $\text{Fe}^{3+}$ .  $\text{Fe}^{3+}$  privileges the coordination of the lactam groups in VCL, as both homopolymeric and anionic Mn gels are able to retain iron at neutral pH. Moreover, in PBS buffer,  $\text{Fe}^{3+}$  is still coordinated within the network at neutral pH, whilst  $\text{Mg}^{2+}$  at the same medium is not bonded at all (see Table S5, ESI†). The number of metal ions ( $\text{Mg}^{2+}$ ,  $\text{Sr}^{2+}$  and  $\text{Cu}^{2+}$ ) that are coordinated by the microgels is dependent on the number of COOH groups, and the COOH/ $\text{M}^{n+}$  ratio is about 2, which makes it straightforward to predict the amount of metal bonded for each sample. In contrast,  $\text{Fe}^{3+}$  might interact also with the lactam monomers of the microgel, however, preferring the lactam group as the bonding cannot be described as easily anymore.<sup>31</sup> Furthermore, Fig. 4 shows that the COOH groups become dominant in the coordination of  $\text{Fe}^{3+}$  only at higher mol%, since the amount of  $\text{Fe}^{3+}$  bonded is comparable to the remaining ions. Leaching experiments were performed to test the stability of the metal ion–microgel systems. In fact, if the bonding affinity is too low, the gel will lose metal overtime, until an equilibrium is reached. The affinity towards the COOH groups has an impact on how well the system can retain the given ion, when the microgel system is subjected to mechanical stress and changes in the external environment. In Fig. 5, the amount of  $\text{Mg}^{2+}$  (Fig. 5a) and  $\text{Fe}^{3+}$  (Fig. 5b) is plotted against centrifugation and dispersion cycles. Alkaline earth metals tend to go into solution when the gels have been freshly loaded, and it takes a couple of washing cycles until no metal is released anymore. This suggests that the  $\text{Mg}^{2+}$  amount that is withheld within the network is lower than the measured metal concentration at the pure first uptake. This means that the metal ion–gel system under mechanical stress such a centrifugation

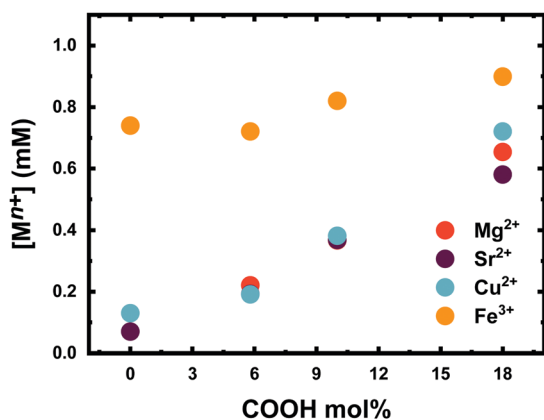


Fig. 4 Concentration of  $\text{Mg}^{2+}$ ,  $\text{Sr}^{2+}$ ,  $\text{Cu}^{2+}$  and  $\text{Fe}^{3+}$  bonded by a 0.1 wt% microgel solution with different COOH mol% per gel: N0 (0 mol% COOH), M1 (5.8 mol% COOH), M2 (10 mol% COOH) and M3 (18 mol% COOH) at RT and neutral pH.

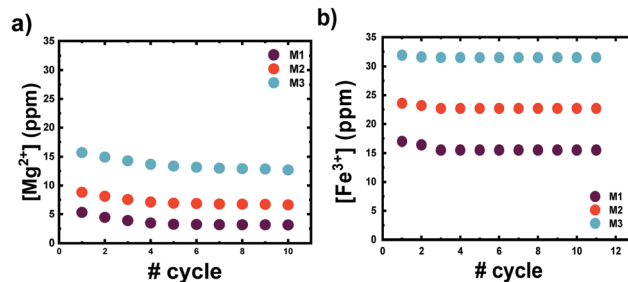


Fig. 5 Amount of (a)  $\text{Mg}^{2+}$  and (b)  $\text{Fe}^{3+}$  retained in a 0.1 wt% microgel system at neutral pH and RT when subjected to consecutive cycles of centrifugation and dispersion in MilliQ water.

requires an excess of COOH to withhold the alkaline earth metals if their affinity is relatively low. In a previous report, we have shown that  $\text{Ca}^{2+}$  was fully retained in the network, due to its extremely high binding strength to COOH, coupled to a possible favourable charge correlation effect.<sup>25,36</sup> The microgels seem to retain much better the transition metal ions, where no leaching is observed at all. The metal ions bind typically to the carboxyl groups. Hence, a full or partial protonation of the carboxyl groups should disrupt the metal–ligand interaction and the metal is released from the microgel. In all cases as depicted in Fig. 6, the pH required to release the metal ions in solution is below 3, with a high release percentage at pH 2. A small release of ions is observed at pH 5 and 4, where only a few of the COOH moieties are protonated. No real difference is observed between the cations at this point, except  $\text{Fe}^{3+}$ , which is released at pH 2 only partially.

Therefore, it confirms also the ability of  $\text{Fe}^{3+}$  to bind non-selectively to the microgel. The  $\text{Fe}^{3+}$  ions bonded to the COOH are released, whilst the remaining ions are maintained within the polymer chains. As it is also apparent from Fig. 4,  $\text{Fe}^{3+}$  ions do not only interact with the charged moieties of the polymer

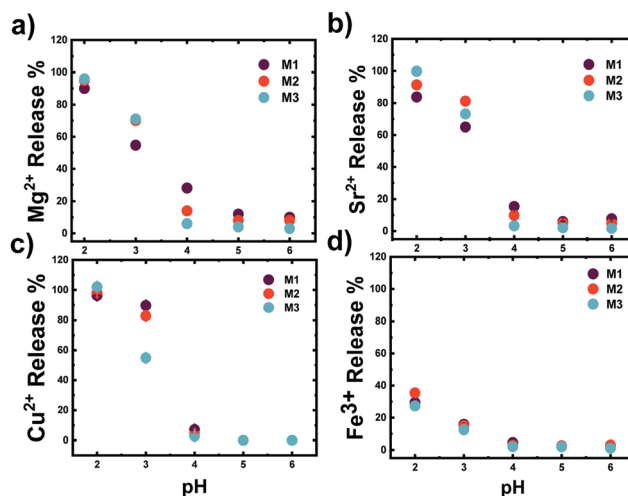


Fig. 6 Percentage of released (a)  $\text{Mg}^{2+}$ , (b)  $\text{Sr}^{2+}$ , (c)  $\text{Cu}^{2+}$  and (d)  $\text{Fe}^{3+}$  by a 0.1 wt% solution of M1 (5.8 mol% COOH), M2 (10 mol% COOH) and M3 (18 mol% COOH) at different pH values at room temperature after an equilibration time of 2 h after pH switch from pH 7.

network but also bond to the lactam groups, where even the neutral microgel N0 is able to retain  $\text{Fe}^{3+}$  within its network.<sup>37,38</sup> This might be accountable to the lactim tautomers present within the network. The local acidity within the bulk of the microgel could lead to a shift of the equilibrium to the lactim form of the monomer, which is capable of coordinating  $\text{Fe}^{3+}$ . Decreasing the pH of the system has an effect on two equilibria: the  $\text{COO}^-$  ions are protonated into  $\text{COOH}$  groups and the lactam tautomerization is pushed towards a higher amount of lactims. Since  $\text{Fe}^{3+}$  is not capable of bonding  $\text{COOH}$  moieties, it will either be released in solution or be coordinated by the lactim moieties. This should explain why there is only partial release of the  $\text{Fe}^{3+}$  ions in solution.

### Reversibility experiments

The gels can uptake and release metal ions “on demand”, without undergoing erosion. To confirm the reversibility of the microgel system over several cycles, the gels were subjected to cycles of loading and unloading of a model ion. The ion chosen was  $\text{Mg}^{2+}$  due to its role in biological processes, which might lead to bioinspired materials.<sup>39,40</sup> In fact, the presence of  $\text{Mg}^{2+}$  triggers the polymerization of G-actin to F-actin also at low pH, and thus the formation of the cytoskeleton.<sup>28</sup> The gels were subjected to 3 cycles of ion addition to the network and pH triggered release, and full loading and unloading could be reached only when the pH was equilibrated back to pH 7. The system is very sensitive to pH changes and ionic strength. These two factors must be controlled, otherwise the loading/release of cations will be strongly affected. Fig. 7 displays the amount of  $\text{Mg}^{2+}$  that a 0.1 wt% microgel solution can load, under ambient conditions and no added salts. The pH is reduced to 2 (data point no. 2 in Fig. 7), to ensure the complete protonation of the  $\text{COOH}$  groups in the system to trigger the release of  $\text{Mg}^{2+}$  ions. Once the pH is equal to 2, the measured quantity of cations remaining in the polymer matrix is close to zero. Full reversibility of the system is ensured by increasing the pH back to neutral whilst keeping the ionic strength low, which involves the use of pure MilliQ water and no base addition. The addition of a base, such as  $\text{NaOH}$  for instance, can disrupt the stability of the gel. It increases the ionic strength of the solution leading to the collapse of the gels as previously described in Fig. 3. The presence of  $\text{NaOH}$  might accelerate the hydrolysis of the crosslinker, which is composed of amide bonds, which are sensitive to high pH. Thus, a reversible loading can be ensured only by switching the pH down to 2, and then increasing it *via* dilution, and not counter titration with a strong base.

### Competition among metal ions

The versatility of a gel system also consists of its ability to selectively bond one metal ion rather than another. An extensive number of examples of polymers were decorated with  $\text{COOH}$  moieties that are able to bond toxic ions like  $\text{Pb}^{2+}$  and  $\text{Hg}^{2+}$ . Nevertheless, removing less toxic ions such as  $\text{Cu}^{2+}$  or  $\text{Fe}^{3+}$  normally only involves the use of  $\text{EDTA}$ .<sup>4</sup> For this reason, here we investigate the competition between ions that are normally removed with  $\text{EDTA}$ :  $\text{Mg}^{2+}$ ,  $\text{Sr}^{2+}$ ,  $\text{Cu}^{2+}$  and  $\text{Fe}^{3+}$ . The selectivity

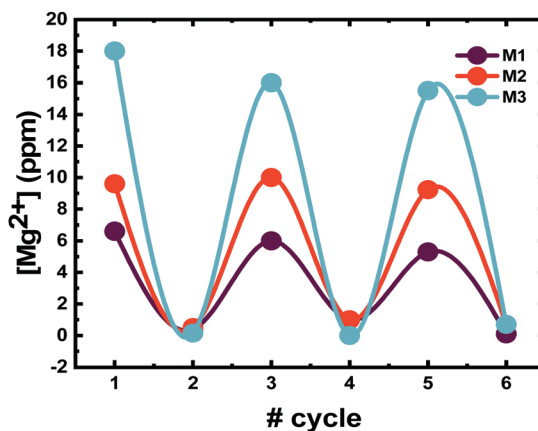


Fig. 7  $\text{Mg}^{2+}$  concentration of M1 (5.8 mol%  $\text{COOH}$ ), M2 (10 mol%  $\text{COOH}$ ) and M3 (18 mol%  $\text{COOH}$ ) 0.1 wt% microgel solutions at room temperature. Odd data points on the x axis represent the loaded amount of  $\text{Mg}^{2+}$  within the total amount of microgels (1, 3, 5) and the remaining even data points refer to the  $\text{Mg}^{2+}$  concentration left within the gel sample after pH trigger (2, 4, 6).

depends on the chemistry of the polymeric chain, which affects bonding sites and accessibility of the sites themselves. The microgel network is composed of VCL moieties and a varying amount of carboxylic acid that comes from the hydrolysed IADME copolymerized within the polymer chains and acts as the cation trap, and the binding strength between the metal ions and the carboxyl groups was investigated.

The different affinity of the metal ion in the presence of another one with the polymer matrix is depicted in Fig. 8 and 9. Fig. 8 focusses on the competition between  $\text{Mg}^{2+}$ ,  $\text{Sr}^{2+}$  and  $\text{Cu}^{2+}$ , whilst Fig. 9 shows the competition between the above-mentioned ions with  $\text{Fe}^{3+}$ . In this figure, two metal ions at the same starting concentration are mixed together in the presence of microgels. The greater the affinity that a cation has with the gel matrix, the greater is the probability that the gel network will retain the cation.<sup>41</sup> By comparing the two alkaline earth ions, these tend to equally distribute within the network, as shown in Fig. 8. On the other

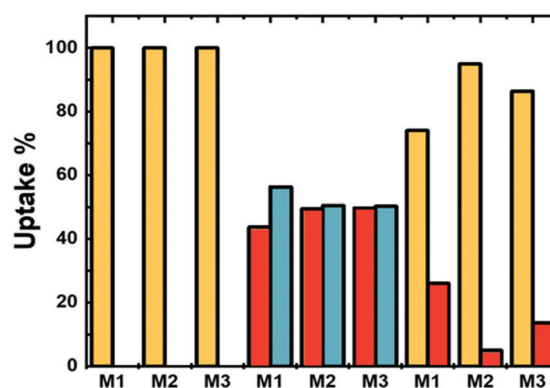


Fig. 8 Percentage of coordinated ions with respect to its competitor for each microgel, M1, M2 and M3, at pH 7 and room temperature. Colour coding: yellow is assigned to  $\text{Cu}^{2+}$ , red to  $\text{Sr}^{2+}$  and green to  $\text{Mg}^{2+}$ . The microgels used are M1 (5.8 mol%  $\text{COOH}$ ), M2 (10 mol%  $\text{COOH}$ ), M3 (18 mol%  $\text{COOH}$ ) and M3 (18 mol%  $\text{COOH}$ ).



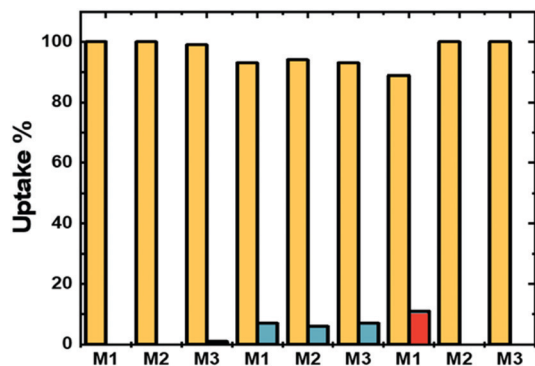


Fig. 9 Percentage of Fe<sup>3+</sup> (in yellow) bonded by a 0.1 wt% microgel solution at pH 7 and room temperature in the presence of Mg<sup>2+</sup> (not visible, first 3 data sets for M1, M2 and M3), Cu<sup>2+</sup> in green and Sr<sup>2+</sup> in red. The microgels used are M1 (5.8 mol% COOH), M2 (10 mol% COOH) and M3 (18 mol% COOH).

hand, the binding affinity with the polymer network is greater for a transition metal ion, when mixed with an alkaline earth cation. As a result, the latter remains in solution. As Sr<sup>2+</sup> binds slightly stronger to the COOH moieties than Mg<sup>2+</sup>, there is not a 100% uptake of Cu<sup>2+</sup>. In the previous section, only one ion at the time was loaded, and all of them showed the same coordination number to the network, implying that each ion, regardless of its nature, employs the same amount of coordination moieties. Hence, by comparing the molar amount of ions taken up by the network, their sum of the two ions is equivalent to the amount of one single ion measured during the uptake experiments. Therefore, no overloading of the system is observed, in any case. As a matter of fact, when the affinity to the network exceeds by far the rest of the ions, such as in the case of Fe<sup>3+</sup>, there is a complete selective uptake of the metal, in the same amount observed as if the Fe<sup>3+</sup> was alone (Fig. 9). In this way, the system can target one ion in particular, which for microgels M1, M2 and M3 is Fe<sup>3+</sup> when under aqueous ambient conditions. Moreover, increasing the ionic strength of the solution by switching the solvent from pure water to PBS does not affect the uptake of Fe<sup>3+</sup> (see Table S5 in the ESI†).

## Conclusions

In this work, the uptake quantification and selectivity towards several cations of a P(VCL-co-IA-co-IADME) microgel system are presented. Three different microgels have been synthesized with respectively 5, 10 and 18 mol% of carboxyl groups, and fully characterized, *via* <sup>1</sup>H NMR, TEM, DLS, SLS and potentiometric titration. The behaviour of each gel has been studied in the presence of 4 multivalent cations: Mg<sup>2+</sup>, Sr<sup>2+</sup>, Cu<sup>2+</sup> and Fe<sup>3+</sup>. The swelling behaviour of the microgels has been first investigated in the presence of a single cation in solution first. The systems appear to have a rather stronger change in size in the presence of the transition metals Cu<sup>2+</sup> and Fe<sup>3+</sup>, whilst the network collapse region remains unvaried regardless of the ion present in solution, be it alkaline earth or transition metal. Furthermore, the possibility of using the cations as cargoes so that they can be coordinated up and released under a pH

trigger has been studied. All cations are released at extremely low pH, and only partial or no release of the cations is observed at neutral pH or pH above 4.5. Otherwise, the binding of ions is prevented, when PBS is used as solvent instead of pure water, suggesting that the release of alkaline earth ions can also be triggered by increasing extensively the ionic strength of the solution. Fe<sup>3+</sup>, on the other hand, does not seem to respond to the ionic strength changes in the medium, and can be bonded with the gel matrix with the same efficiency as in pure water. To determine whether there is a preference of the network for a certain ion, competition experiments have been performed, and a clear selectivity towards Fe<sup>3+</sup> has been observed. The microgels have also been proved to be capable of undergoing multiple cycles of loading and release of their cargo, given that the external conditions, as in ionic strength, are highly controlled. For further investigations, these gels could also be tested for highly poisonous transition ions, such as Hg<sup>2+</sup> or Pb<sup>2+</sup>, that could be removed from the body by sole ingestions of the gels and subsequent expulsion from the digestive system.

## Conflicts of interest

There are no conflicts to declare.

## Acknowledgements

We gratefully acknowledge financial support from the Swiss National Science Foundation, NCCR-MSE and University of Basel. The authors are thankful to Ms Judith Kobler Waldis (University of Basel) for the ion chromatography measurements.

## Notes and references

- 1 J. Anastassopoulou and T. Theophanides, in *Bioinorganic Chemistry: An Inorganic Perspective of Life*, ed. D. P. Kessissoglou, Springer, Netherlands, Dordrecht, 1995, pp. 209–218.
- 2 S. J. Stohs and D. Bagchi, *Free Radicals Biol. Med.*, 1995, **18**(2), 321–336.
- 3 G. Papanikolaou and K. Pantopoulos, *Toxicol. Appl. Pharmacol.*, 2005, **202**(2), 199–211.
- 4 A. Fulgenzi and M. E. Ferrero, *Int. J. Mol. Sci.*, 2019, **20**(5), 1019.
- 5 H. A. Leitch and N. Gattermann, *Crit. Rev. Oncol. Hematol.*, 2019, **141**, 54–72.
- 6 R. S. Britton, K. L. Leicester and B. R. Bacon, *Int. J. Hematol.*, 2002, **76**(3), 219–228.
- 7 M. J. Brown, T. Willis, B. Omalu and R. Leiker, *Pediatrics*, 2006, **118**(2), e534–e536.
- 8 S. R. Karamched, N. Nosoudi, H. E. Moreland, A. Chowdhury and N. R. Vyavahare, *Sci. Rep.*, 2019, **9**(1), 1–11.
- 9 S. Varma and S. B. Rempe, *Biophys. Chem.*, 2006, **124**(3), 192–199.
- 10 M. R. Truter, *Alkali Metal Complexes with Organic Ligands*, Springer, 1973, pp. 71–111.





- 11 M.-O. M. Piepenbrock, G. O. Lloyd, N. Clarke and J. W. Steed, *Chem. Rev.*, 2010, **110**(4), 1960–2004.
- 12 W. Weng, J. B. Beck, A. M. Jamieson and S. J. Rowan, *J. Am. Chem. Soc.*, 2006, **128**(35), 11663–11672.
- 13 P. Innocenzi, *The Sol to Gel Transition*, Springer, 2019, pp. 1–6.
- 14 T. Nakamura, Y. Takashima, A. Hashidzume, H. Yamaguchi and A. Harada, *Nat. Commun.*, 2014, **5**, 4622.
- 15 Q. Lin, B. Sun, Q. P. Yang, Y. P. Fu, X. Zhu, T. B. Wei and Y. M. Zhang, *Chem. – Eur. J.*, 2014, **20**(36), 11457–11462.
- 16 B. O. Okesola and D. K. Smith, *Chem. Soc. Rev.*, 2016, **45**(15), 4226–4251.
- 17 A. M. Atta, H. S. Ismail and A. M. Elsaad, *J. Appl. Polym. Sci.*, 2012, **123**(4), 2500–2510.
- 18 J. Y. Lim, S. S. Goh, S. S. Liow, K. Xue and X. J. Loh, *J. Mater. Chem. A*, 2019, **7**(32), 18759–18791.
- 19 T. C. Tseng, L. Tao, F. Y. Hsieh, Y. Wei, I. M. Chiu and S. h. Hsu, *Adv. Mater.*, 2015, **27**(23), 3518–3524.
- 20 L. Shi, P. Ding, Y. Wang, Y. Zhang, D. Ossipov and J. Hilborn, *Macromol. Rapid Commun.*, 2019, **40**(7), 1800837.
- 21 J. Li and D. J. Mooney, *Nat. Rev. Mater.*, 2016, **1**(12), 1–17.
- 22 F. A. Plamper and W. Richtering, *Acc. Chem. Res.*, 2017, **50**(2), 131–140.
- 23 W. Xu, A. A. Rudov, R. Schroeder, I. V. Portnov, W. Richtering, I. I. Potemkin and A. Pich, *Biomacromolecules*, 2019, **20**(4), 1578–1591.
- 24 A. P. Gelissen, A. Scotti, S. K. Turnhoff, C. Janssen, A. Radulescu, A. Pich, A. A. Rudov, I. I. Potemkin and W. Richtering, *Soft Matter*, 2018, **14**(21), 4287–4299.
- 25 F. Horkay, I. Tasaki and P. J. Bassar, *Biomacromolecules*, 2001, **2**(1), 195–199.
- 26 V. Chimisso, C. Fodor and W. Meier, *Langmuir*, 2019, **35**(41), 13413–13420.
- 27 L. Etchenausia, E. Villar-Alvarez, J. Forcada, M. Save and P. Taboada, *Mater. Sci. Eng., C*, 2019, **104**, 109871.
- 28 M. Carlier, D. Pantaloni and E. Korn, *J. Biol. Chem.*, 1987, **262**(7), 3052–3059; L. M. Gaetke and C. K. Chow, *Toxicology*, 2003, **189**(1–2), 147–163.
- 29 A. Balaceanu, D. E. Demco, M. Möller and A. Pich, *Macromolecules*, 2011, **44**(7), 2161–2169.
- 30 S. Schachsal, A. Balaceanu, C. Melian, D. E. Demco, T. Eckert, W. Richtering and A. Pich, *Macromolecules*, 2010, **43**(9), 4331–4339.
- 31 D. W. Yin, F. Horkay, J. F. Douglas and J. J. de Pablo, *J. Chem. Phys.*, 2008, **129**(15), 154902.
- 32 G. S. Longo, M. Olvera de La Cruz and I. Szleifer, *Macromolecules*, 2011, **44**(1), 147–158.
- 33 M. Mussel and F. Horkay, *J. Phys. Chem. Lett.*, 2019, **10**(24), 7831–7835.
- 34 P. K. Jha, J. W. Zwanikken, J. J. De Pablo and M. O. De La Cruz, *Curr. Opin. Solid State Mater. Sci.*, 2011, **15**(6), 271–276.
- 35 W. N. Sharratt, R. O'Connell, S. E. Rogers, C. G. Lopez and J. T. Cabral, *Macromolecules*, 2020, **53**(4), 1451–1463.
- 36 M. Mussel, P. J. Bassar and F. Horkay, *Soft Matter*, 2019, **15**(20), 4153–4161.
- 37 M. Zabiszak, M. Nowak, K. Taras-Goslinska, M. T. Kaczmarek, Z. Hnatejko and R. Jastrzab, *J. Inorg. Biochem.*, 2018, **182**, 37–47.
- 38 G. Maistralis, N. Katsaros, S. P. Perlepes and D. Kovala-Demertzi, *J. Inorg. Biochem.*, 1992, **45**(1), 1–12.
- 39 V. Gal, S. Martin and P. Bayley, *Biochem. Biophys. Res. Commun.*, 1988, **155**, 1464–1470.
- 40 D. Meksuriyen, T. Fukuchi-Shimogori, H. Tomitori, K. Kashiwagi, T. Toida, T. Imanari, G. Kawai and K. Igarashi, *J. Biol. Chem.*, 1998, **273**(47), 30939–30944.
- 41 G. M. Eichenbaum, P. F. Kiser, D. Shah, W. P. Meuer, D. Needham and S. A. Simon, *Macromolecules*, 2000, **33**(11), 4087–4093.

